Chapter 5

Ion Beams for Nanoscale Optical Data Storage

Tania Tsvetkova

Additional information is available at the end of the chapter

http://dx.doi.org/10.5772/intechopen.77976

Abstract

The ion beam techniques have been investigated as a novel approach for properties modification and optimization of wide-bandgap materials with view of their uses in submicron lithography and high-density data storage for archival purposes. Focused ion-implantation has been used to write nanoscale optical data into wide-bandgap amorphous materials (hydrogenated amorphous silicon carbide (a-SiC:H) and tetrahedral amorphous carbon (ta-C) films). Scanning near-field optical microscopy is proposed as a novel technique for characterizing the ion-implanted patterns fabricated in amorphous silicon carbide (a-SiC:H). Although a considerable thickness change (thinning tendency) has been observed in the ion-irradiated areas, the near-field measurements confirm increases of optical absorption in these areas. The results are discussed in terms of the competition between the effects of ion implantation and surface milling by the ion beam. The observed effects are important for amorphous silicon carbide and tetrahedral amorphous carbon thin films as extremely stable materials in adverse environments to be used for permanent data archiving. The observed values of the optical contrast modulation are sufficient to justify the efficiency of the method for optical data recording using focused ion nanobeams.

Keywords: focused ion beams, optical data storage, data archiving, ion beam lithography, wide-bandgap amorphous materials

1. Introduction

The use of ion beam techniques is a very attractive method to modify and control material properties [1]. A major aim of materials research has been to develop new solid media and working tools. Joint efforts by industry and research institutions have advanced the use of these developments in the important social area of information technology serving many

fields of our social and cultural life. In these computer-related technologies, rapidly advancing progress has always demanded improved solutions for mass data storage.

Present-day digital memories are subject to lifetime limitations of the order of some 10 years due to physico-chemical deterioration effects at ambient temperatures, so that an enormous effort in continuously rewriting library archives onto freshly prepared media is anticipated. This is true for both recording techniques presently in main use: magnetic and optical disks are affected by thermal, mechanical and chemical events. In addition, magnetic information can also be destroyed by electromagnetic fields. Thus, for cultural values of all kinds to be preserved for future generations, other ways have to be found providing unlimited lifetimes. Safe archival data storage has become an urgent issue. Electronic libraries already constitute an important issue in this field. Foreseeable total storage volumes approach the order of 1 Eb, or 10^{18} b. Thus, it is of paramount interest to find a truly permanent recording technology with the additional condition of higher storage density. The steadily increasing amount of digital data of global order of zetta bytes will require novel storage techniques of ultra-high density, possibly in the nanoscale [2].

The main aim of this chapter is to present some novel approaches to this problem. The reading of such digital data with nanometer dimensions is also subject to further technical progress. In this chapter, how ion nanobeams are used to write data bits of nanometer diameter into new generation storage materials is presented and photon near-field technology is employed to read this novel kind of digital memory.

2. Optical contrast formation in wide-bandgap materials

During many years of development, ion beams have found important applications to the modification of materials. While ion-implantation technology has revolutionized the industrial production of electronic devices, optical applications have so far been scarce. This state of affairs is quite astonishing, since optical changes in certain wide-bandgap materials, in particular in semiconductors, are very pronounced and easily produced. Both physical processes and applications to the optical modification of certain insulators have been reviewed in a dedicated publication by Townsend et al. [3].

Recently, ion beam-induced optical modification of wide-bandgap materials has been successfully employed for the development of novel methods for high-density data storage [4, 5]. There have been two markedly different kinds of approaches: a method based on ion beam-induced amorphization of wide-bandgap crystalline materials [4] and a method based on ion beam optical modification of wide-bandgap amorphous materials [5], both using highly focused ion nanobeams.

2.1. Ion beam-induced amorphization of wide-bandgap crystalline materials

The optical properties of crystalline insulating materials can markedly be modified by irradiation with energetic ions. Radiation damage causes dramatic changes of the optical absorption in the bandgap energy regime of crystalline insulating materials. In particular, if the state of amorphicity can be introduced, absorption changes will be strongest. The exposed areas of

such materials absorb and reflect light more strongly than non-irradiated ones. In this way, optical contrast is created between irradiated and non-irradiated areas, if suitable masks are applied or alternatively, computer-controlled focused ion beam (FIB) equipment is used [6].

With modern equipment, ion beams of sufficient intensity can be focused to submicron dimensions. Thus, both analog and digital information can be recorded with pixel densities of Gbit/cm^2 to Tbit/cm^2. Initially, focused ion beams of inert gas ions (Ar^+, Ne^+, Xe^+), produced by gas-field ion sources (GFIS), were employed to generate optical patterns of both kinds in wide-bandgap crystalline materials. This is demonstrated in **Figure 1**, showing digital data storage (ionographic process) in crystalline films of group-IV elements of the periodic system and in **Figure 2**, where analog information storage in polycrystalline silicon carbide (pc-SiC) by focused Ne^+ beam is presented. Usually, this type of optical data storage is read in light transmission mode (**Figure 3**), hence highly transparent optical substrates are used, like Al_2O_3 (sapphire).

Crystalline films of group-IV elements of the periodic system, such as Si, SiC and C_D (diamond), are best suited for this novel data recording process, due to the marked differences in their absorption coefficient in the two different phases—crystalline and amorphous (**Figure 4**). As shown, due to their higher bandgap energies, the optical "contrast window" for SiC and C_D (diamond) is shifted toward the ultra-violet part of the spectrum.

2.2. Ion beam modification of wide-bandgap amorphous materials

Since the crystalline-amorphous contrast-based data storage in thin film crystalline materials is usually read in light transmission mode, it requires the use of solid transparent substrates, for example, quartz or sapphire that meet certain requirements. To produce analog patterns in pc-Si on sapphire written by focused Ar^+ or Ne^+ beam (**Figure 2**) the procedure starts first with plasma deposition of a-SiC:H film with moderate absorption. To achieve the needed initial high film transparency for the aimed high optical contrast after irradiation, the next step is

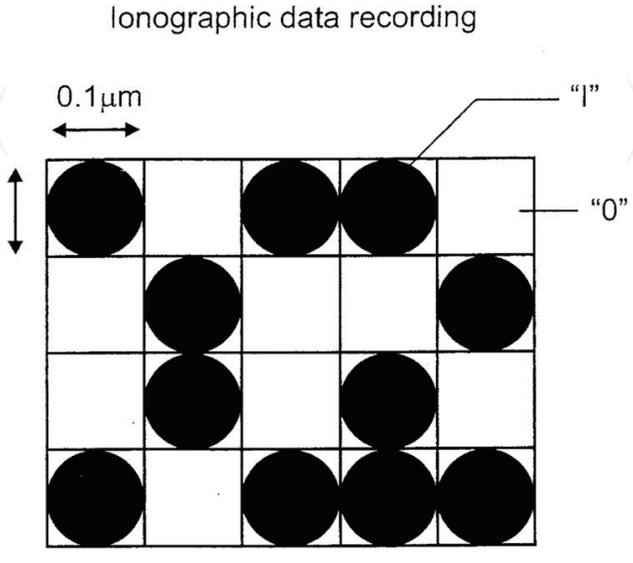

Figure 1. Crystalline-amorphous digital pattern obtainable by writing with a focused ion beam into a thin film of Si, SiC or C_D [5].

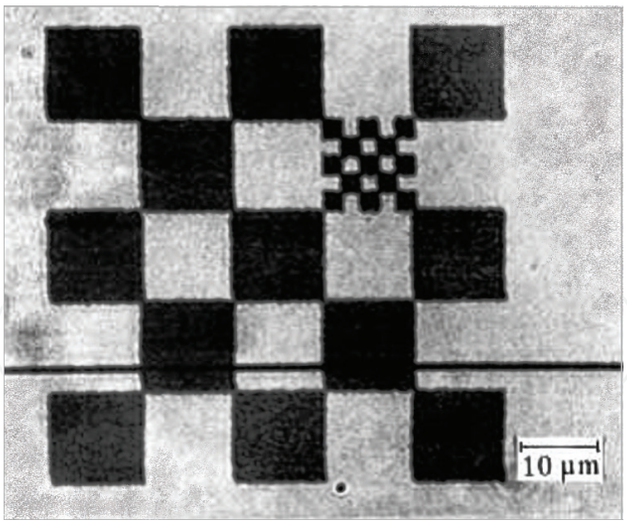

Figure 2. Crystalline-amorphous analog pattern in poly-crystalline SiC on a sapphire substrate by using a 20 keV focused Ne beam [5].

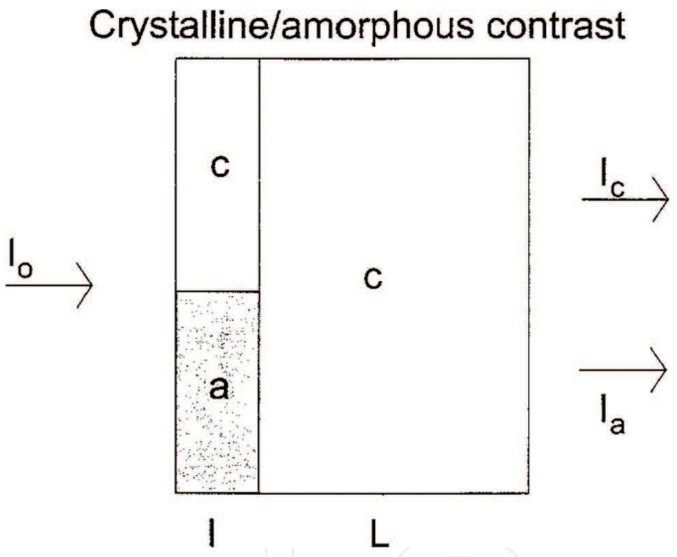

Figure 3. Principle of crystalline-amorphous contrast. Incident light of intensity I_0 traverses a thin layer l of material consisting of crystalline and amorphous areas on a thick transparent substrate. The transmitted beams I_c and I_a have different intensities [5].

to produce low absorption pc-SiC by crystallizing the a-SiC:H film in a special hot furnace at temperatures as high as 1400°C. This high temperature requires the use of high-quality expensive sapphire substrates. Only after this costly technological step the ion irradiation is performed to achieve the aimed optical contrast (**Figure 5**) and generate optical information patterning of the pc-SiC (**Figure 2**) [7].

On the other hand, although these investigations have shown the feasibility of this method for achieving the initially stated goals for permanent safe archival dense data storage, it has been stressed that the whole process requires also further high-technology processing steps, for example, the use of Ar^+, Ne^+ and Xe^+ nanobeams of nA intensity, the equipment systems

http://dx.doi.org/10.5772/intechopen.77976

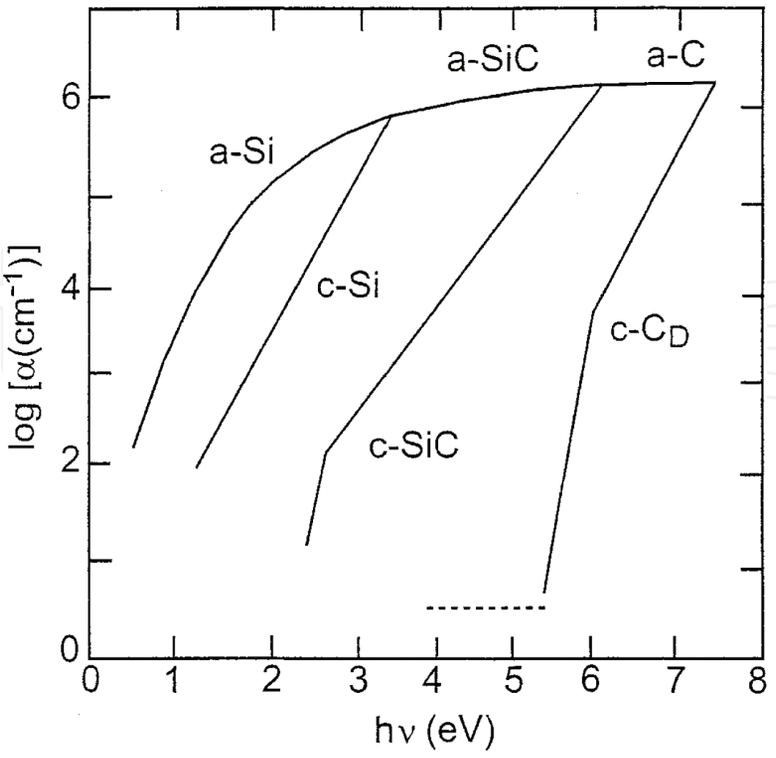

Figure 4. Working range of different group-IV semiconductors for crystalline-amorphous contrast. Note that the amorphous phases follow a common curve, whereas the crystalline phases are distinctly different [5].

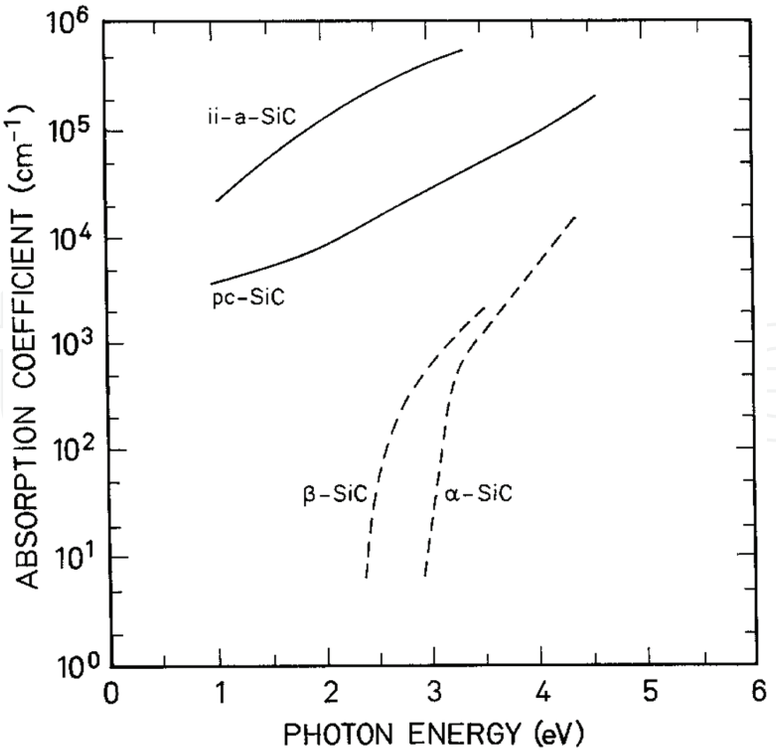

Figure 5. Optical absorption coefficient of SiC films (full lines) as obtained after poly-crystallization (pc-SiC) and irradiation with Ar^+ ions (ii-a-SiC). The dashed lines refer to monocrystalline α- and β-SiC [5].

for which are rare to find. The authors have admitted that such equipment is not yet commercially available even though, depending on the importance of the respective data, costs nevertheless look affordable [8].

The above costly requirements have been later avoided with the development of yet another optical data storage method, using the ion beam-induced optical contrast in wide-bandgap amorphous materials by their structural-and chemical-based optical modification. Previous investigations of Tsvetkova et al. [9] on the optical effects of Ar^+, N^+ and O^+ bombardment of thin chalcogenide films of the As-Se system at comparable implantation conditions, have shown that the chemically active N^+ and O^+ species have a more pronounced effect on the optical characteristics of the films, even though Ar^+ has a higher mass and hence would yield higher amounts of radiation defects. The effect of the higher changes in the absorption coefficient and refractive index, induced by the N^+ and O^+ implantation as compared to the Ar^+ bombardment, has been attributed, apart from the increased amount of radiation defects, also to their chemical modification by reacting with the As-Se host atoms and creating new bonds, affecting the amorphous material electronic structure and hence modifying the optical properties.

In the case of the a-SiC:H amorphous material, used as a source material for the crystallization step to produce a highly transparent pc-SiC film and thus achieve maximum optical contrast with the Ar^+ ion irradiated a-SiC, a new route has been suggested to avoid the crystallization step and start with as transparent as possible initial a-SiC:H material even though it will be somewhat less transparent than the pc-SiC. Indeed, the optical bandgap width of a-$Si_{1-x}C_x$:H is known to be easily controlled by controlling its stoichiometry (x) and may vary between 1.8 and 3.0 eV [10].

On the other hand, for the achieved optical contrast, it is not the absolute values of the optical absorption of the initial material and the irradiated one but the relative difference between the two absorption coefficients. Thus, even though this coefficient for the starting a-SiC:H material is higher than the one for pc-SiC, if the ion irradiated a-SiC:H can be rendered still more absorbing by using instead of Ar^+ bombardment some more chemically effective ion species, competing results can be easily achieved with the ones for the method based on crystalline-amorphous contrast. Such chemically active dopants have been known to be Ge and Sn, effectively reducing the optical bandgap of a-SiC:H, when added during the deposition process [11].

A considerably higher optical effect has been achieved in a-SiC:H films by ion implantation of Ge and Sn as compared to the effect of Ar bombardment [12], as shown in **Figure 6**. (The sample preparation conditions of the a-SiC:H films for this study, together with the parameters of the ion implantation processing of the samples employed, are described elsewhere [12, 13]; it is worth though to mention here that simple Corning glass was used for the transparent substrates instead of sapphire.) This effect is manifested by an optical transmission edge shift to the larger wavelengths, accompanied by a decrease in the transmission coefficient, as a result of the ion implantation.

The registered difference in the optical effect for the three types of ions is attributed to the different chemical nature of the implanted elements rather than to the radiation effect difference due to the varying parameters of the implanted species. This has been ensured by

http://dx.doi.org/10.5772/intechopen.77976

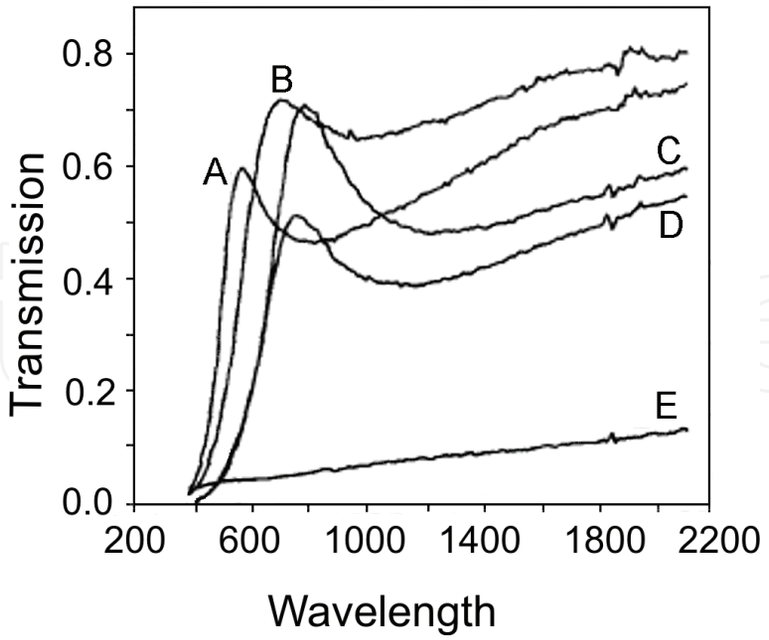

Figure 6. Transmission spectra of unimplanted (A) and implanted with Ar^+, Ge^+ and Sn^+ at D = 10^{17} cm^{-2} (spectra B, D and E, respectively) and with Sn^+ at D = 10^{16} cm^{-2} (C) a-$Si_{0.82}$ $C_{0.18}$:H films [12].

	Ar	Ge	Sn
E (keV)	30	50	75
R_p (nm)	37.1	34.3	38.0
ΔR_p (nm)	14.8	12.1	11.5

Table 1. Energies, normalized projected range R_p and standard deviation ΔR_p for the three types of implanted ions [12].

an appropriate choice of the film thickness (d = 100 nm) and ion energies, so as to match the resulting projected ranges R_p and standard deviation ΔR_p for the three elements, as estimated approximately using LSS theory and SRIM program [14]. (See **Table 1** [12]).

Figure 7 demonstrates the changes of the absorption coefficient α with the dose both for Ge^+ and Sn^+ (**Figure 7a** and **b**, respectively) implantation in a-SiC:H films. It is easily noticed that the ion implantation increases α and shifts the absorption edge to the lower energies even for the lowest dose (D = 10^{15} cm^{-2}). Saturation is reached gradually when increasing the dose. Determination of the absorption coefficient α for the highest implantation dose of Sn^+ (D = 10^{17} cm^{-2}) is hampered by the drastic decrease of transmission (**Figure 6**), related to certain metallization in this case, and hence it is not presented in the figure.

The results for the dose dependence of the Tauc optical gap E_g for the cases of ion implantation with Ge^+ and Sn^+ are shown in **Table 2** [12].

The observed optical properties modification effects induced by the ion implantation of a-SiC:H films signify a change in the energy spectrum of the electronic states. The observed change could be related to breaking of bonds and increase of disorder due to ion bombardment for the three elements (Ar, Ge and Sn), and for the case of Ge and Sn—also to some

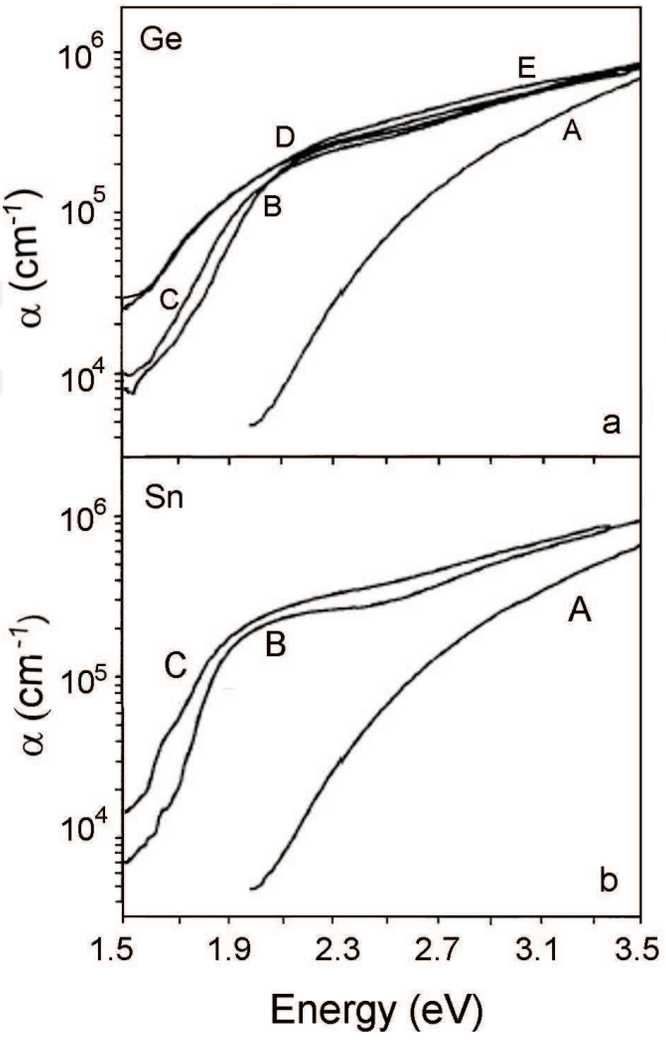

Figure 7. Absorption coefficient α of unimplanted (A) and implanted with Ge^+ (a) and Sn^+ (b) a-$Si_{0.82}C_{0.18}$:H films at doses (in cm^{-2}): 10^{15}(B), 10^{16}(C), 5×10^{16}(D) and 10^{17}(E) [12].

Eg [eV]				
	x = 0.18		**x = 0.35**	
D [cm^{-2}]	**Ge**	**Sn**	**Ge**	**Sn**
0	2.08	2.08	2.32	2.32
1×10^{15}	1.64	1.66	2.05	1.85
1×10^{16}	1.58	1.53	1.99	1.77
5×10^{16}	1.22	—	1.83	0.89
1×10^{17}	1.22	—	1.68	0.23

Table 2. Tauc optical gap E_g of Ge^+ and Sn^+ implanted a-$Si_{1-x}C_x$:H films with different carbon content (x = 0.18 and x = 0.35) at different doses [12].

accompanying formation of additional bonds between the implanted ions and the atoms of the alloy host material, as confirmed by vibrational spectroscopy (IR and Raman) [13], X-ray photoelectron spectroscopy (XPS) [15] and Mössbauer spectroscopy analysis [16].

http://dx.doi.org/10.5772/intechopen.77976

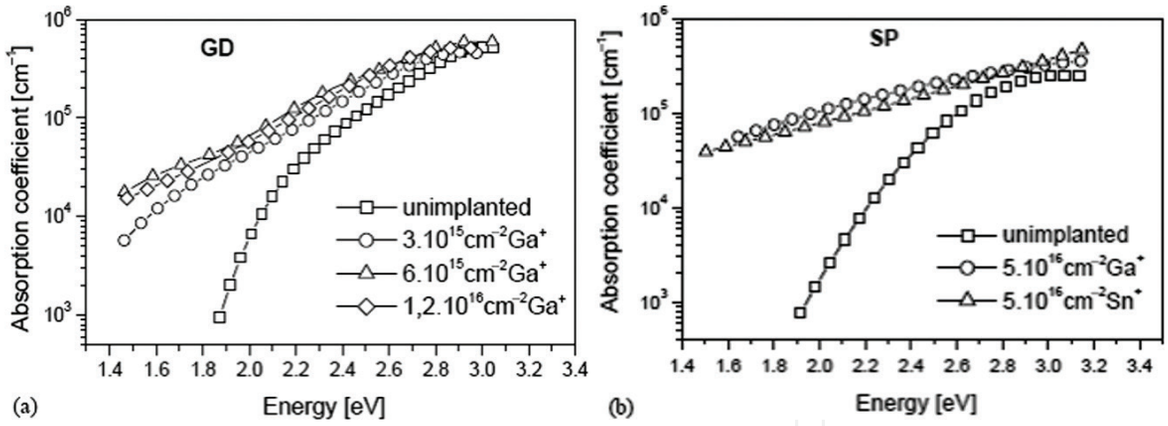

Figure 8. Absorption coefficient α of a-$Si_{1-x}C_x$:H (x = 0.15) films implanted with: (a) Ga^+ at a dose $D_1 = 3 \times 10^{15}$ cm^{-2}, $D_2 = 6 \times 10^{15}$ $cm^{-2}$and $D_3 = 1.2 \times 10^{16}$ cm^{-2}; (b) Ga^+ and Sn^+ at a dose $D = 5 \times 10^{16}$ cm^{-2} [17].

As has been noted about the results presented in **Figure 7**, they clearly show that the ion implantation of Ge and Sn in a-SiC:H films increases α and shifts the absorption edge to the lower energies even for the lowest dose ($D = 10^{15}$ cm^{-2}) and saturation is reached gradually when increasing the dose. Thus, the absorption coefficient change may reach ~ 2 orders of magnitude in the visible light range of the spectrum even applying quite moderate ion doses, allowing for a choice of lower ion doses aiming at a reduced cost. However, to proceed to optical patterning of a-SiC by focused Ge^+ or Sn^+ ion beams, some specially designed focused ion beam (FIB) systems have to be used. And although such custom-built Ge^+ and Sn^+ FIB systems do exist and are available at request, it appeared desirable to explore the possibility to use instead the much more widely spread commercial FIB systems, using Ga^+ focused ion beams for patterning.

Hence, further experiments were focused on the achievable optical contrast in a-SiC:H films by Ga^+ ion implantation, using a wide range of ion doses [17]. The results are presented in **Figure 8**, which clearly shows that the optical effects for the Ga^+ implantation are comparable with the ones for Ge^+ and Sn^+ for similar range of ion doses (**Figure 8b**). It is also demonstrated that for the case of Ga^+ as well, lower doses of the order of 10^{15} cm^{-2} may be sufficient to justify the requirements for optical patterning of a-SiC for optical data storage (**Figure 8a**). Possible applications of these results in the area of submicron lithography and high-density optical data archiving have been suggested with regard to the most widely spread focused microbeam systems based on Ga^+ liquid metal ion sources.

3. Optical patterning of wide-bandgap amorphous materials

The work on the optical patterning of wide-bandgap amorphous silicon carbide for nanoscale archival data storage and submicron lithography constitutes a further step to extend the use of optical crystalline materials, as data storage media, to the new class of wide-bandgap amorphous materials with their numerous technological and ecological advantages. It also extends the use of the FIB systems based on gas-field ion sources (GFIS), implemented as a patterning tool, to the use of the more versatile and widespread FIB systems based on liquid-metal ion sources (LMIS), which are also preferred in many practical applications for some of their superior features.

3.1. Focused ion beam (FIB) systems used for nanoscale patterning

Nanoscale focused ion beams (FIBs) represent one of the most useful tools in nanotechnology, enabling nanofabrication via milling and gas-assisted deposition, microscopy and microanalysis and selective, spatially resolved doping of materials. These instrumentation developments, that have come to play a central role in nanotechnology, have made it possible to create a beam of ions focused to a spot size on the order of just a few nanometers [18].

The ion source is a core part of a FIB system, and its function is to produce an ion beam. [19] There are, indeed, various types of ion sources and a wealth of different ion species, some of which are commercially available, and others that exist in custom-built research laboratory setups only, to be used in niche applications or to be further developed. The state of the ion source technology is historically an enabling factor for FIB instruments.

Beginning in the late 1970s, ion sources with the necessary characteristics began to appear, and one type that soon came to dominate was the liquid metal ion source (LMIS).With an extremely simple construction, high brightness and robust performance, the LMIS has become a central driver in the widespread adaptation of focused ion beam techniques in nanotechnology [20].

In the manufacturing process of the LMIS, a tungsten needle with the tip diameter of 5–10 μm can be made by electrochemical corrosion and then adhere molten liquid metal on the tip of tungsten needle. An electric field is applied on the tip; then the liquid metal on the tip is formed to Taylor cone under the strong electric field force. The electric field intensity of Taylor cone can be as high as 10^{10}V/m, and the metal ions in the surface layer of liquid metal would escape in the form of field evaporation, resulting in the ion beam. The schematic diagram LMIS with a two-lens system is presented in **Figure 9**.

Another type of field-ionization sources (discovered earlier than LMIS) is based on ionizing molecules adsorbed from their gas phase. These gas field ion sources (GFIS) are in use for producing ion beams of hydrogen and noble gases by condensing them first, followed by electric field ionization on an atomically sharp needle, this way creating very small (sub-nm) diameter

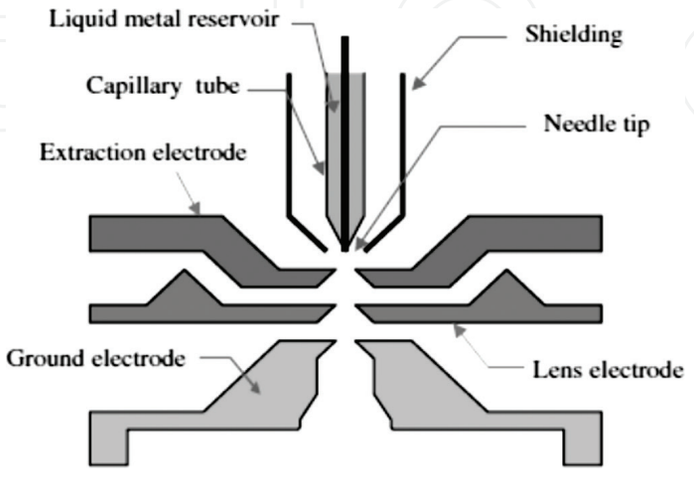

Figure 9. LMIS in a two-lens system.

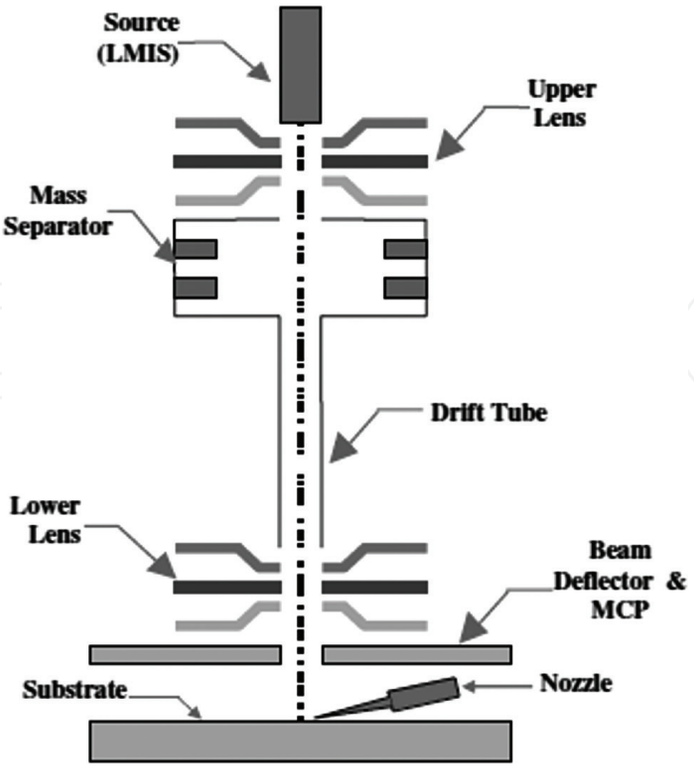

Figure 10. Schematic diagram of LMIS-based FIB.

and small current beams. Major drawback of GFIS though is that it produces very low current on final focal spot [21]. For many practical applications, LMIS-based FIBs are the preferred choice.

The schematic diagram of the LMIS-based FIB is presented in **Figure 10**. The focusing and scanning equipment is generally constituted by a double electricity lens system, beam blanking assembly and quadruple deflection electrode. The sample station includes the sample stage, the detector and the gas injection system. The sample can move along with x, y, z axis, rotate around z axis and move obliquely in five degrees of freedom when it is placed on the stage. In order to improve the controllability and the speed of the nanofabrication, a gas injection system is also introduced in the sample chamber. Further results presented in this work are implemented using the LMIS-based FIB.

3.2. Amorphous silicon carbide and tetrahedral amorphous carbon materials

Hydrogenated amorphous silicon carbide (a-SiC:H) alloy films have great technological potential as structural materials for high-temperature electronics and for various optoelectronic elements and devices designed to operate in aggressive environments (acid vapors, radiation, open space, etc.) [22, 23]. An important feature underpinning the material's environmental robustness is the comparatively wide bandgap which may be tailored in the range 1.8–3.0 eV.

The material can be prepared in thin-film form on different substrates by chemical vapor deposition [24] or by employing a radio-frequency reactive magnetron sputtering method [25]. Reactive sputtering is a convenient method to prepare a-SiC:H films where low-density-of-states

material is not required, as is very often the case. Mechanical, optical and electrical parameters of the material can be controllably varied by changing the relative composition of the constituent elements. In addition, control of electronic and optical properties of such materials can be achieved using ion implantation [26, 27].

Thin films of amorphous carbon (a-C) also referred to as diamond like carbon (DLC), have received considerable attention due to their intrinsic highly attractive properties. Amorphous carbon (a-C) is a disordered phase of carbon without long-range order, containing carbon atoms mostly in graphite-like sp2 and diamond-like sp3 hybridization sites. Depending on the relative concentrations of sp2- or sp3- hybridized carbon, a-C has shown excellent physical properties such as high hardness, low friction coefficient, chemical inertness, relatively high thermal conductivity and optical transparency [28]. The term tetrahedral amorphous carbon (ta-C) is used to describe amorphous carbon films with a large percentage of *sp*3 bonding (up to 87%). The films are manufactured using a variety of techniques, including filtered cathodic vacuum arc (FCVA), pulsed laser deposition (PLD) and mass selected ion beam deposition (MSIBD) [28, 29]. The high *sp*3 content in the films results in unique properties that include extreme hardness (~70 GPa), chemical inertness, high electrical resistivity and wide optical bandgap. These properties also offer some advantages as compared to another wide optical bandgap material—silicon carbide (SiC)—for uses in nanoscale optical data recording for archival information storage using focused ion beams (FIB) techniques.

3.3. FIB optical patterning of a-SiC and ta-C films

The use of ion implantation as a method of introducing additional elements to modify the material chemically and hence its electronic characteristics (the bandgap and the related optical and electrical properties) is an attractive means to control these properties. It is particularly of interest in connection with the emerging techniques of easily operated ion microbeams and the possibilities they reveal for fabricating various sophisticated planar structures [30].

Recently, using the fast developing technology of ion microbeams, promising results have been obtained for the possible application of thin polycrystalline silicon carbide films in high-density optical data storage and submicron lithography [6–8]. This approach has been further developed by implementing ion doping of amorphous silicon carbide films with focused ion beam (FIB) systems that use Ga^+ or other chemically active ion species as implants [12, 17].

The widespread use of FIB systems based on Ga^+ LMIS has prompted special attention to the choice of Ga^+ as the implant species in further experiments. Investigations on Ga^+ broad-beam implanted a-SiC:H films have shown various structural and chemical modification changes, resulting in an effective optical bandgap decrease and considerable optical absorption coefficient increase [17]. The underlying mechanism, as studied by IR and Raman measurements, involves breaking of Si–H and C–H bonds and apparent loss of H. An increased Si–C bond breaking is revealed and formation of Si–Ga bonds, implying that Ga substitutes for the C atom in the C–Si–H bond due its lower electronegativity [31, 32]. Yet, due to the low melting point of Ga (Tm = 29.8°C), some part of the implanted Ga ions are apparently incorporated as Ga-clusters rather than directly bonded to host atoms [33].

The computer-controlled focused ion-beam system IMSA-100 [34] working with a Ga^+ LMIS was used to create a preliminary chosen optical pattern in a-SiC:H films [17]. The

computer-generated pattern, shown in **Figure 11**, consists of several line series and chess-board-type fields with different sizes and doses of implanted Ga^+. The shorter line series LS1 (size 2.5/2.5/20 mm) and the longer ones LS2 (size 5/5/40 mm) were obtained with Ga^+ ion doses in the range $D = 5 \times 10^{15}$–2×10^{17} cm^{-2}. The big chess-board-type field (BCF) (size 20 mm) and the smaller chess-board-type fields SCF1 and SCF2 (size 10 mm) were obtained with doses $d_1 = 2.5 \times 10^{16}$ cm^{-2} (BCF and SCF1) and $d_2 = 4 \times 10^{16}$ cm^{-2} (SCF2). The figure shows the potential of this method for different applications as diverse as high-density optical data storage and direct writing of submicron lithographic masks for microelectronics and optoelectronics.

Similarly, programmable computer-controlled focused ion-beam system, working with a Ga^+ LMIS, was used to create a preliminary chosen optical pattern in ta-C films [35]. Samples of

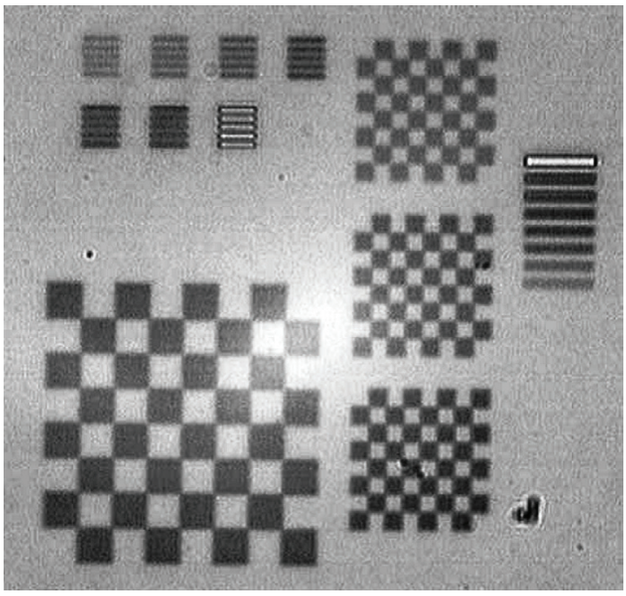

Figure 11. Micron-scale pattern on an a-SiC:H film written with the FIB using a 15 pA Ga^+ − ion beam. The size of the big chess field is 20 × 20 mm^2 [17].

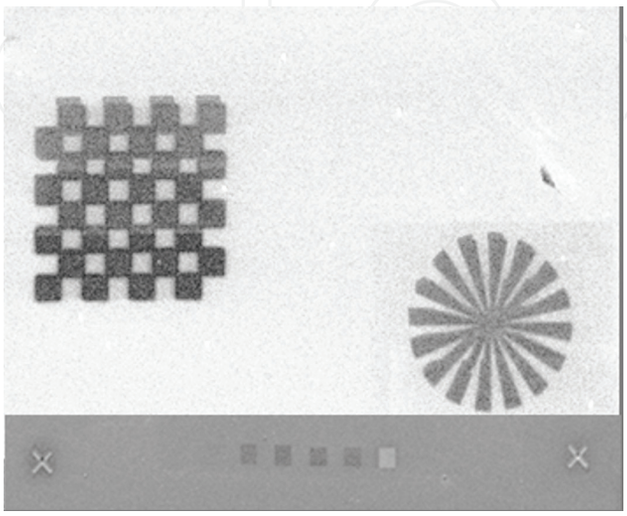

Figure 12. Contrast images in ta-C film, written with the FIB using a 15 pA Ga^+ − ion beam, and dependence of absorbance of implanted areas on Ga^+ fluences (squares 10 × 10 μm^2): 1e14, 5e14, 1e15, 5e15, 1e16, 5e16 cm^{-2} [35].

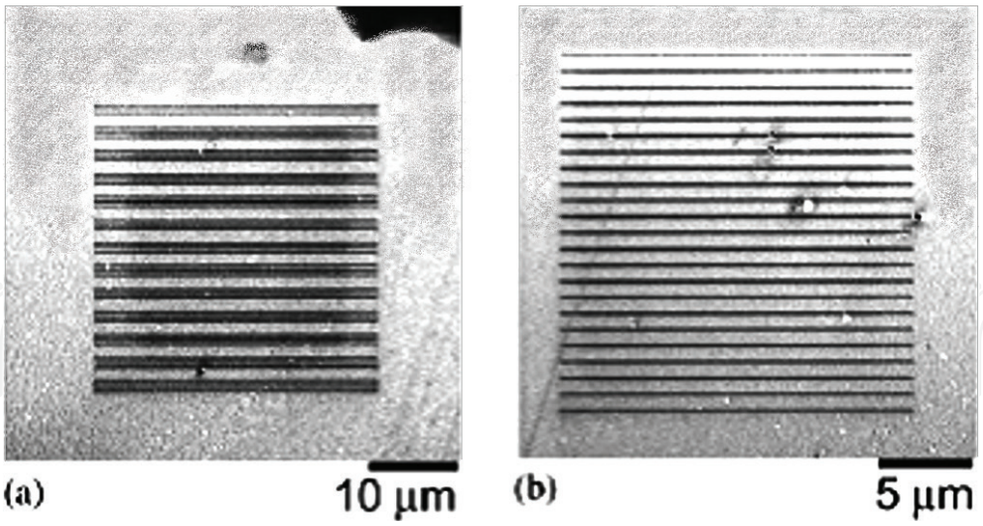

Figure 13. Secondary ion image of (a) triplet lines pattern (100 nm width, 300 nm separation between adjacent lines in each triplet and 1000 nm separation between triplets) and (b) low-density set of single lines (100 nm width and 900 nm separation), in an Al-coated a-SiC:H thin film, written with FIB system using focused Ga^+ ion beam [36].

thin ta-C films (d~40 nm) were deposited on Corning glass substrates using a commercial FCVA system (Commonwealth Scientific Corporation). The Ga^+ focused ion beam (FIB) patterning was performed with NVision 40 Crossbeam System (Zeiss) using 1, 10, 80 pA Ga^+, 30 keV and a range of Ga^+ ion doses (**Figure 12**).

Some further results of the experiments at the nanoscale by patterning a-SiC:H samples with Ga^+ FIB are demonstrated in **Figure 13** [36]. The secondary ion images recorded immediately after the FIB implantation in the vacuum chamber are shown in the figure. Each pattern consists of a set of lines with 100 nm width separated differently. The secondary ion images show that a line thickness as small as 100 nm has been realized.

4. Near-field technique uses for reading nanoscale optical data

The optical properties of nanoscale structures need to be characterized with a "super-resolution" technique, for example, near-field techniques. Additionally, the ion irradiation induced sputtering may cause ablation of the a–SiC:H film, resulting in changes in the surface topographic features. Hence, a technique mapping the topographic features of the patterns, such as atomic force microscopy (AFM) [37, 38], is also needed to characterize the modified surfaces. From these points of view, scanning near-field optical microscopy (SNOM), supplied with shear force technique providing also topographic data, is a promising method that can simultaneously obtain optical and topographic images of the samples [38–41].

Atomic force microscope (AFM) (Dimension 3000 Digital Instruments) was used to analyze the topography of the fabricated patterned samples in these studies [39]. Scanning near-field optical microscope (SNOM) was used to study the changes in local optical absorption of the irradiated (patterned) areas as compared to the nonirradiated ones [42].

A schematic diagram of the SNOM equipment used is presented in **Figure 14** [42]. An unpolarized He-Ne laser (633 nm) beam is used to illuminate the sample from its nonpatterned

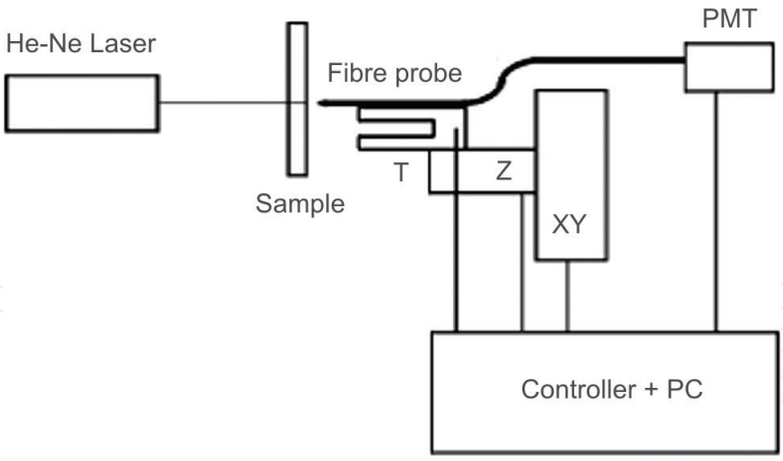

Figure 14. A schematic diagram of SNOM set-up. Photomultiplier tube (PMT); quartz tuning fork (T); piezoelectric stage for scanning (XY); piezoelectric actuator (Z) [42].

side of the transparent substrate. The transmitted light is then collected with a sharpened optical fiber tip positioned in near-field proximity to the patterned surface and is measured with a photomultiplier tube (PMT). The tip is raster scanned across the sample while kept at a constant tip-surface distance, and topographic data and optical images are recorded simultaneously. The tip-surface distance is monitored with nonoptical detection technique using shear-force feedback, where the tip is oscillated by a quartz tuning fork (T) and oscillation amplitude is monitored as variations of the electric impedance of the tuning fork. While the tip scans the sample, the piezoelectric actuator (Z) moves it so as to keep the oscillation amplitude constant, tracing the topography. The typical diameter of the fiber tip end, fabricated by chemical etching, is 100 nm and this determines the optical resolution.

4.1. Atomic force microscopy characterization of FIB patterns

These near-field techniques were used to study Ga^+ FIB patterns in a-SiC:H films [42]. Sample preparation was as follows: thin films of a-$Si_{1-x}C_x$:H (x = 0.15) were deposited by RF (13.56 MHz) reactive magnetron sputtering onto Corning glass substrates. The composite target, comprising of mono-crystalline (100) silicon wafer with chips of pure graphite placed on top, was sputtered in an Ar-20%H_2 gas mixture. The deposition conditions typically were RF power of 150 W, power density 1.91 W/cm^2, total gas pressure 1P, substrate temperature 275°C and graphite-to-silicon target ratio 0.025. Talystep profilometer and optical measurements were used to determine the film thickness d~200 nm. The carbon content (x) of the films was determined by Rutherford backscattering spectrometry (RBS) to be 0.15.

Computer-operated FIB system, using focused Ga^+-ion beam implantation, was applied to produce various pre-designed optical patterns in these samples. The FIB system used was IMSA-Orsay Physics, supplied with a "charge neutralizer" (e^- beam shower). The obtained patterns are presented in **Figure 11**. The figure represents an optical micrograph of a a-SiC:H thin film with a variety of FIB-created patterns. They consist of chess-board-like (CBL) patterns and series of lines with different doses (SL). The optical density of the irradiated areas is increased due to the ion implantation; hence, they are seen as dark regions.

Topographic images of the irradiated areas were recorded with AFM before conducting the SNOM experiments. The results for the recorded CBL and SL structures are shown in **Figure 15**.

The AFM analysis of these results reveals that the irradiated areas are topographically lower. This is supposedly due to the ion beam-induced ablation of the thin film. A cross-sectional view of the AFM image of a SL is presented in **Figure 15(b)**. The dose of the ions is highest on the left-hand side (3.2×10^{16} cm^{-2}), decreasing toward the right-hand side (0.8×10^{15} cm^{-2}). The higher doses are shown to cause larger variations of the topography, as expected.

4.2. Scanning near-field optical microscopy (SNOM) of FIB patterns

As already mentioned in the previous paragraph, SNOM can provide simultaneously an optical image of the corresponding topographic image. As a demonstration of its potential, CBL patterns with different doses are investigated with SNOM. The obtained topographic data and corresponding optical images are demonstrated in **Figure 16**. Compared with the unpatterned areas at the left-hand side of the image, the areas irradiated with ion beam are topographically lower, while being optically more opaque. The observed trend of the topographic features of the irradiated areas are the same as that observed with the AFM (cf. **Figure 15**), while the observed trend of optical contrasts obtained with SNOM is qualitatively the same as that obtained with conventional optical microscopy (cf. **Figure 11**).

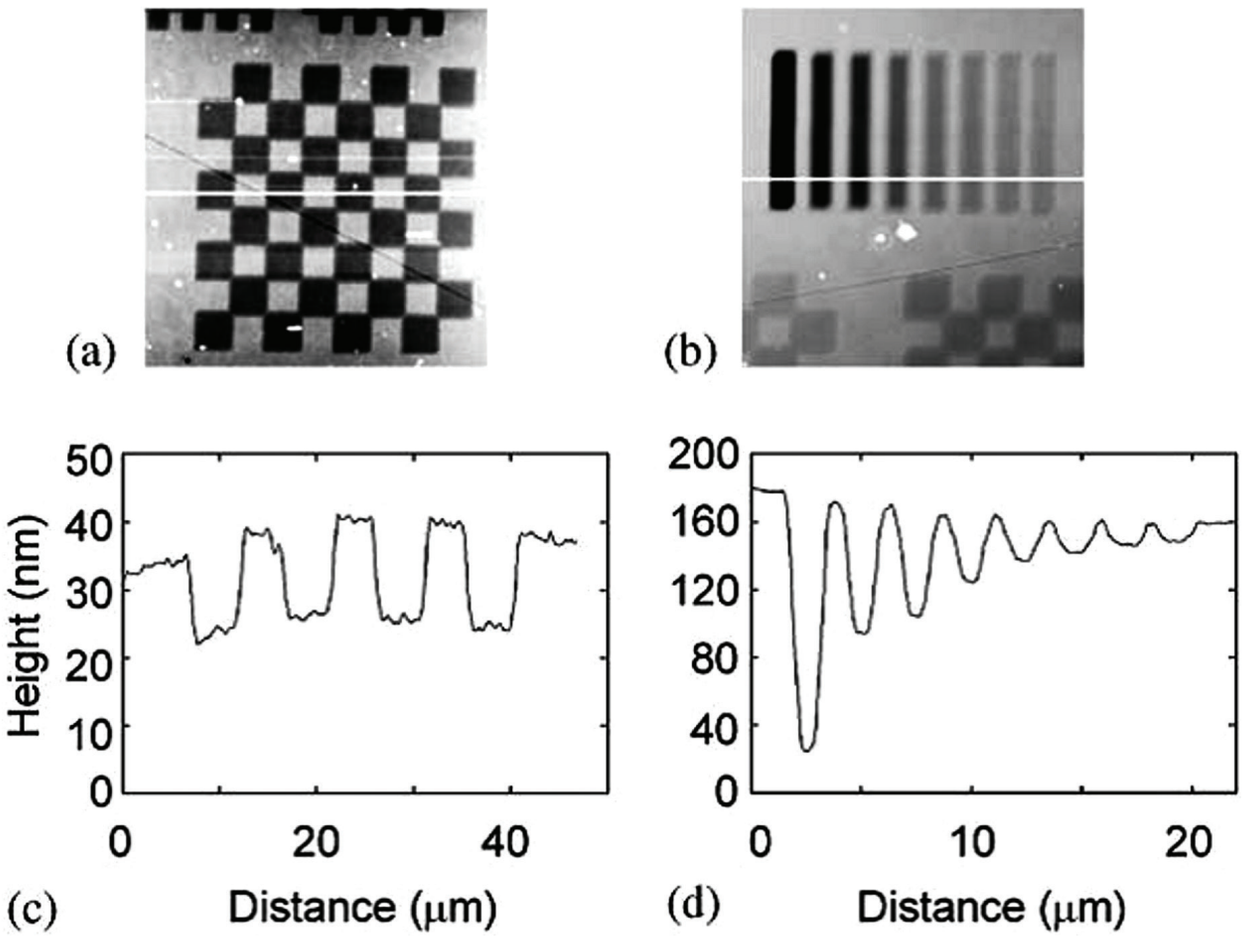

Figure 15. AFM images of (a) CBS and (b) SSL patterns in an a-SiC:H film fabricated by the irradiation of focused ion beam. The cross sections indicated in (a) and (b) are shown in (c) and (d), respectively [42].

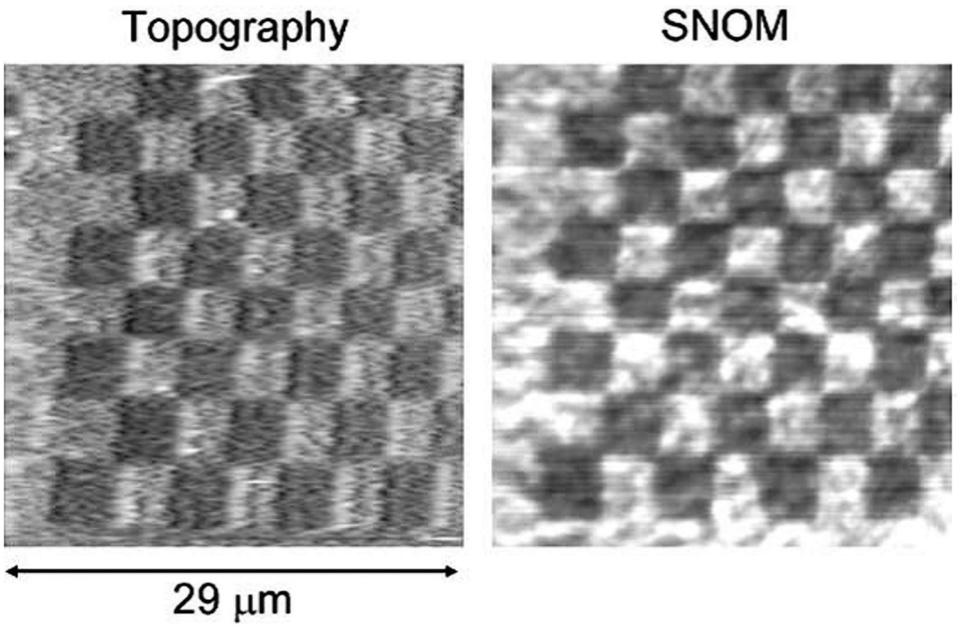

Figure 16. Topographic image (a) and corresponding SNOM image (b) of a CBS pattern created on an a-SiC:H thin film [42].

For the purpose of examining the dependencies of topographic and optical contrasts on the Ga^+ ion dose, three different CBL patterns with doses of 1.3×10^{16}, 0.8×10^{16} and 3.2×10^{15} cm^{-2} have been scanned with SNOM to record topographic and optical images. The obtained results are presented in **Figure 17**. The topographic thickness changes (thinning) of the CBL patterns are measured to be 90, 80 and 50 nm for Ga^+ doses of 1.3×10^{16}, 0.8×10^{16} and 3.2×10^{15} cm^{-2}, respectively. The measured corresponding optical contrasts are 0.5, 0.4 and 0.2. It is thus shown that it can be qualitatively concluded that a higher dose causes both higher optical and higher topographic contrast. It has to be noted, though, that this correlation is an average one, for example, in **Figure 17(C)**, the CBL pattern in the optical image is smeared, while topographic features are still being observed. Since the value of the lowest optical contrast of 0.2 obtained here is rather high, the inhomogeneous optical images of **Figure 17(C)** may be attributed to the inhomogeneous optical property of the material due to contamination or some interference effects associated with the formation of two-dimensional periodic structures. Such information can be used to set optimal dose condition to achieve maximum optical contrast with minimum topographic contrast and less artificial optical features.

4.3. Optimal optical contrast in FIB-patterned amorphous silicon carbide structures

The optical density of ion implanted regions is determined by two competing contributions, mechanical thinning of the a–SiC:H film due to ion beam milling and modification of the film properties (i.e. increased optical absorption) due to ions implanted in the film. Thus, studies of both topographic and optical properties of thin films are important to optimize the ion implantation processing for optical data storage applications. Such investigations have been carried out by simultaneous mapping of topography and optical contrast of Ga^+ FIB optical stripes patterns in a-SiC:H with varying ion dose using a SNOM instrument [43].

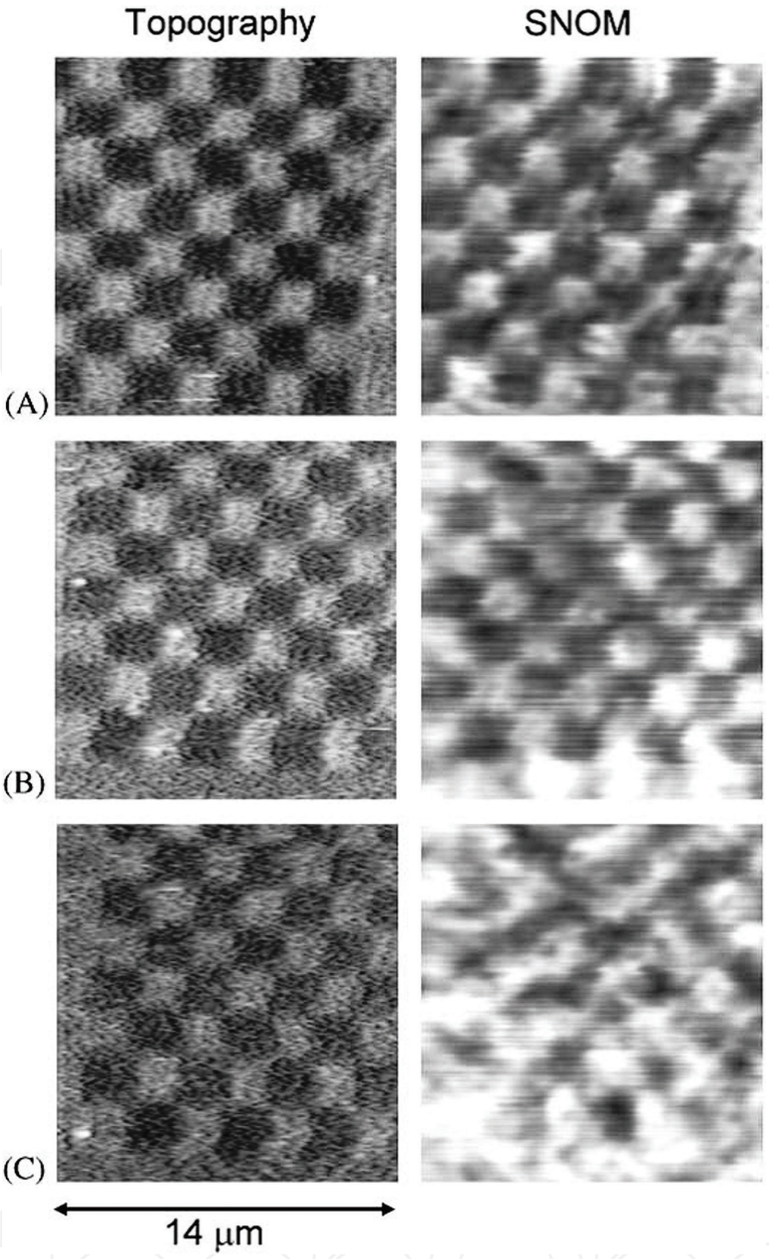

Figure 17. Variations of topographic and near-field optical contrasts of CBL patterns fabricated with different ion doses: (A) 1.3×10^{16} (B) 0.8×10^{16} and (C) 3.2×10^{15} cm^{-2} [42].

When irradiating a film surface with a beam of accelerated ions, there are two main possible processes involved: implantation of the ions into the film [1, 3] and ablation of the film [1, 44]. The resulting increase of optical density in a-SiC:H is assumed to be caused by the former process, while topographic thinning results from the latter. The maximum optical absorption that can be developed in the film may also be limited by the ablation since sputtering of gallium will define an upper limit to the amount that is retained. Effectively, the number of ions per volume implanted into the irradiated material increases with the dose to a certain saturation point, limited by the ion beam-induced sputtering. At the same time, the amount of film material sputtered away from the solid surface increases with the dose as long as the irradiation continues. The results presented in the work of Takahashi et al. [43] show that at

lower doses the ion implantation prevails over the ablation effect. The implantation effect reaches saturation at a dose $D = 3.0 \times 10^{15}$ ions cm^{-2}. Then, for higher irradiation doses, the ablation effect starts to override the implantation effect, leading to a slow decrease in the optical contrast, while the topographic thinning still increases.

The key feature which must be noted for a practical device is not the level of absorption achieved by the implant, but the contrast that develops relative to the immediately adjacent regions. Local optical measurements as in this work [43] are of particular importance in this respect as they provide a way to study how sharp the optical contrast change is between the implant zones and nominally unaffected regions between them. It is also noted there, in way of comparison, that the change in the optical absorption in this case is somewhat less than the order of magnitude change obtained in conventional far-field optical measurements in samples implanted with an unfocused, broad ion beam [17]. The large optical contrast in the far-field optical measurements case arises mainly from amorphization changes in the host material, but these are less important here; instead, the transmission changes are more strongly defined by the presence of Ga itself and the formation of nanoscale precipitates [33]. Moreover, surface temperature enhanced sputtering (including that of the Ga implant) from the ion beam irradiated regions will act to limit the transmission change achievable.

5. Conclusions

The results presented here demonstrate the possibility to open up new applications of wide bandgap amorphous materials, such as a-SiC:H and ta-C, as media for high-density optical data storage in the nanoscale range, using focused ion beam techniques. In summary, the optical contrast achieved, even at relatively low doses, is of sufficient magnitude to be useful in nanoscale optical data storage and submicrometer lithographic mask production. These results are particularly important when estimating the cost effectiveness of the method, as relatively low implantation doses appear effective in this case and these imply less costly implantation time. The resolution achievable will be defined by the diameter of the Ga^+ FIB and the region of collateral modification/damage, similar to proximity effects in the case of electron beam patterning, but still should offer a significant improvement over the resolution determined by the diffraction limit of light in the case of optical lithography.

Applying near-field optical techniques, like SNOM, for optical and topographic characterization of Ga^+ FIB patterned surfaces, provided results showing that at lower doses, the ion implantation effect leads to increased optical absorption and, hence, higher optical contrast is dominant. However, the optical absorption saturates at higher implantation doses while further ion beam milling causes a decrease in optical contrast, apparently due to the ablation of the film. Thus, the present study shows the existence of optimal conditions for the ion implantation to achieve large optical contrast with less topographic change in the films. Low ion irradiation doses are effectively sufficient and preferable for achieving strong modification of the optical absorption, which is needed for applications in optical data storage for creating permanent optical archives. The obtained results, given the potential of the FIB technique, could be of use for applications of wide-bandgap amorphous materials, like a-SiC and ta-C, in the area of nanoscale optical data storage and data archiving.

Acknowledgements

The support of the Bulgarian Academy of Sciences and Maria Curie-Sklodowska University in Lublin, Poland, is gratefully acknowledged, as well as the help of the staff of the Ion Beam Center at the Helmholtz-Zentrum Dresden-Rossendorf e.V., a member of the Helmholtz Association, for performing the focused ion beam implantation.

Author details

Tania Tsvetkova

Address all correspondence to: tsvet@issp.bas.bg

Institute of Solid State Physics, Bulgarian Academy of Sciences, Sofia, Bulgaria

References

[1] Townsend PD, Kelly JC, Hartley NEW. Ion implantation, sputtering and their applications. London: Academic Press Inc. Ltd; 1976

[2] The Digital Universe of Opportunities. April 2014. Available: www. emc.com/digital universe

[3] Townsend PD, Chandler PJ, Zhang I. Optical effects of Ion Implantation. Cambridge: University Press; 1994. pp. 24-55

[4] Kalbitzer S. Novel concepts for the mass storage of archival data. Nuclear Instruments and Methods B. 2004;**218**:343-354

[5] Tsvetkova T. Ion beam modification of amorphous silicon-carbon alloys. In: Singh J, Copley S, Mazumder J, editors. Beam Processing of Advanced Materials. ASM International: Metals Park. 1996. p. 207

[6] Kalbitzer S. Generation of optical contrast in insulating materials by irradiation with focused ion beams. Applied Physics A. 2000;**71**:565-569

[7] Ruttensberger B, Krotz G, Muller G, Derst G, Kalbitzer S. Crystalline-amorphous contrast formation in thermally crystallized SiC. Journal of Non-Crystalline Solids. 1991;**137-138**:635

[8] Kalbitzer S. High density optical memories for safe archival data. Physical Science International Journal. 2014;**4**(3):366-371

[9] Tsvetkova T, Amov B, Vateva E, Averyanov V. Ion implantation induced modification of vitreous chalcogenides. Physica Status Solidi (a). 1990;**119**:107

[10] Bullot J, Schmidt MP. Physics of amorphous silicon-carbon alloys. Physica Status Solidi (b). 1987;**143**:345

[11] Demichelis F, Kaniadakis G, Tagliafero A, Tresso E, Rava P. Amorphous hydrogenated silicon-carbon-tin alloy films. Physical Review B. 1988;**37**:1231

[12] Tsvetkova T, Tzenov N, Tzolov M, Dimova-Malinovska D, Adriaenssens G, Pattyn H, Lauwerens W. Optical contrast formation in a-$Si_{1-x}C_x$:H films by ion implantation. Journal of Non-Crystalline Solids. 1993;**164-166**:897

[13] Tzenov N, Tzolov M, Dimova-Malinovska D, Tsvetkova T, Angelov C, Adriaenssens G, Pattyn H. Ion implantation induced modification of a-SiC:H. Nuclear Instruments and Methods B. 1994:**84**:195

[14] SRIM by Ziegler JF, Biersack JP, Ziegler MD. University of California at Los Angeles. CA 90066; 2012 (Available: www.SRIM:org.)

[15] Tzenov N, Dimova-Malinovska D, Tsvetkova T. Modification of magnetron sputtered a-Si_{1-x} C_x:H films by implantation of Sn^+. Materials Research Society Symposia Proceedings. 1996;**396**:243

[16] Barancira T, Moons R, Koops CEJ, Deweerd W, Pattyn H, Tzenov N, Tzolov M, Dimova-Malinovska D, Tsvetkova T, Venegas R, Zhang GL. Study of the ion implantation of ^{119}Sn in a-$Si_{1-x}C_x$:H. Journal of Non-Crystalline Solids. 1999;**244**:189

[17] Bischoff L, Teichert J, Kitova S, Tsvetkova T. Optical pattern formation in a-SiC:H films by Ga^+ ion implantation. Vacuum. 2003:**69**:73

[18] McClelland JJ, Steele AV, Knuffman B, Twedt KA, Schwarzkopf A, Wilson TM. Bright focused ion beam sources based on laser-cooled atoms. Applied Physics Reviews. 2016:**3**(1):011302: DOI: 10.1063/1.4944491

[19] Giannuzzi LA, Stevie FA. In: Introduction to Focused Ion Beams. New York: Springer; 2005

[20] Tseng AA. Recent developments in micromilling using focused ion beam technology. Journal of Micromechanics and Microengineering. 2004;**14**:R15-R34

[21] Nabhiraj PY, Menon R, Mohan Rao G, Mohan S, Bhandari RK. Characterization of compact ICP ion source for focused ion beam applications. Nuclear Instruments and Methods in Physics Research A. 2010;**621**:57-61

[22] Powell JA, Matus L. In: Harris GL, Yang CYW, editors. Amorphous and Crystalline Silicon Carbide. Berlin: Springer; 1989

[23] Kanicki J, editor. Amorphous and Microcrystalline Semiconductor Devices. Boston. London: Artech House; 1991

[24] Heinrich J, Hemeltjen S, Marx G. Analytics of CVD Processes in the deposition of SiC by methyltrichlorosilane. Microchim Acta. 2000;**133**:209

[25] Nagai T, Yamamoto K, Kobayashi I. SiC thin-film thermistor. Journal of Physics E. 1982;**15**:520

[26] Hirvonen JK. Ion implantation and ion beam processing of materials. Amsterdam: North Holland; 1984

[27] Ziegler JF. Ion implantation. New York: Academic Press; 1988

[28] Veerasamy VS, Yuan J, Amaratunga G, Milne WI, Gilkes KWR, Weiler M, Brown LM. Nitrogen doping of highly tetrahedral amorphous carbon. Physical Review B. 1993; **48**:17954

[29] Fallon PJ, Veerasamy VS, Davis CA, Robertson J, Amaratunga GAJ, Milne WI, Koskinen. Properties of filtered-ion-beam-deposited diamondlike carbon as a function of ion energy. Journal of Physical Review B. 1993;**48**:4777

[30] Böhringer K, Jousten K, Kalbitzer S. Development of a high- brightness gas field-ionization source. Nuclear Instruments and Methods B. 1988;**30**:289

[31] Tsvetkova T, Tzenov N, Tzolov M, Dimova-Malinovska D, Adriaenssens GJ, Pattyn H. Optical properties and chemical structure of ion implanted a-SiC:H. Vacuum. 2001;**63**:749

[32] Tsvetkova T, Angelov O, Sendova-Vassileva M, Dimova-Malinovska D, Bischoff L, Adriaenssens GJ, Grudzinski W, Zuk J. Structural and optical properties modification of a-SiC:H by Ga+ ion implantation. Vacuum. 2003;**70**:467

[33] Hole DE, Townsend PD, Barton JD, Nistor LC, Landuyt J. Gallium colloid formation during ion implantation of glass. Journal of Non-Crystalline Solids. 1995;**180**:266-274

[34] Bischoff L, Hesse E, Panknin D, Skorupa W, Teichert J. Writing implantation with a high current density focused ion beam. Microelectronic Engineering. 1994;**23**:115

[35] Tsvetkova T, Berova M, Sandulov M, Kitova S, Avramov L, Boettger R, Bischoff L. Focused ion beam optical patterning of ta-C films. Surface and Coatings Technology. 2016;**306**:341-345

[36] Tsvetkova T, Takahashi S, Zayats A, Dawson P, Turner R, Bischoff L, Angelov O, Dimova-Malinovska D. Fabrication of nano-scale optical patterns in amorphous silicon carbide with focused ion beam writing. Vacuum. 2005;**79**:100-105

[37] Binnig G, Quate CF, Gerber Ch. Atomic Force Microscope. Physical Review Letters. 1986;**56**:930

[38] Friedbacher G, Fuchs H. Classification of scanning probe microscopies. Pure and Applied Chemistry. 1999;**71**:1337

[39] Betzig E, Trautman JK. Near-field optics: microscopy, spectroscopy, and surface modification beyond the diffraction limit. Science. 1992;**257**:189

[40] Pohl DW, Courjon D, editors. Near Field Optics. Dordrecht: Kluwer Academic Publishers; 1993

[41] Richards D, Zayats AV, editors. Nano-optics and near-field microscopy. Philosophical Transactions of the Royal Society. London: 2004;**362**:699-812

[42] Tsvetkova T, Takahashi S, Zayats A, Dawson P, Turner R, Bischoff L, Angelov O, Dimova-Malinovska D. Near-field optical mapping of the ion-implanted patterns fabricated in amorphous silicon carbide. Vacuum. 2005;**79**:94-99

[43] Takahashi S, Dawson P, Zayats AV, Bischoff L, Angelov O, Dimova-Malinovska D, Tsvetkova T, Townsend PD. Optical contrast in ion-implanted amorphous silicon carbide nanostructures. Journal of Physics D: Applied Physics. 2007;**40**:7492-7496

[44] Knystautas E, editor. Engineering Thin Films and Nanostructures with Ion Beams. Boca Raton, FL: Taylor and Francis; 2005

IntechOpen